Drug and Alcohol Dependence 145 (2014) 134–142

Contents lists available at ScienceDirect

Drug and Alcohol Dependence

journal homepage: www.elsevier.com/locate/drugalcdep

Characterizing white matter changes in cigarette smokers via diffusion tensor imaging

Ricky R. Savjani[a], Kenia M. Velasquez[b], Daisy Gemma Yan Thompson-Lake[b], Philip Rupert Baldwin[b], David M. Eagleman[a,b], Richard De La Garza II[a,b], Ramiro Salas[b,*]

[a] Department of Neuroscience, Baylor College of Medicine, One Baylor Plaza, Houston, TX 77030, United States
[b] Menninger Department of Psychiatry and Behavioral Sciences, Baylor College of Medicine, One Baylor Plaza, Houston, TX 77030, United States

ARTICLE INFO

Article history:
Received 8 August 2014
Received in revised form
18 September 2014
Accepted 4 October 2014
Available online 22 October 2014

Keywords:
TBSS
Probabilistic tractography
DTI
Tobacco
Nicotine
Cigarette

ABSTRACT

Background: Tobacco use remains the most preventable cause of death; however, its effects on the brain, and particularly white matter, remain elusive. Previous diffusion tensor imaging (DTI) studies have failed to yield consistent findings, with some reporting elevated measures of fractional anisotropy (FA) and others reporting lowered FA.
Methods: In our study, we sought to elucidate the effects of tobacco on white matter by using enhanced imaging acquisition parameters and multiple analysis methods, including tract-based spatial statistics (TBSS) with crossing fiber measures and probabilistic tractography.
Results: Our TBSS results revealed that chronic cigarette smokers have decreased FA in corpus callosum and bilateral anterior internal capsule, as well as specific reduced anisotropy in the two major fiber directions in a crossing fiber model. Further, our tractography results indicated that smokers have decreased FA in tracts projecting to the frontal cortex from (1) nucleus accumbens, (2) habenula, and (3) motor cortex. We also observed that smokers have greater disruptions in those regions when they had recently smoked compared to when they abstained from smoking for 24 h. Our results also support previous evidence showing hemispheric asymmetry, with greater damage to the left side compared to the right.
Conclusions: These findings provide more conclusive evidence of white matter disruptions caused by nicotine use. By better understanding the neural disruptions correlating with cigarette smoking we can elucidate the addictive course and explore targeted treatment regimens for nicotine dependence.
Published by Elsevier Ireland Ltd.

1. Introduction

Although the effects of cigarette smoking have been well studied in several model systems, the effects of chronic tobacco use on brain structures have not been well characterized. Particularly, diffusion tensor imaging (DTI) has yielded inconsistent findings on white matter structural changes caused by nicotine use. Some data indicate chronic cigarette smoking increases fractional anisotropy (FA) in several white matter regions, including bilateral frontoparietal regions (Liao et al., 2011), portions of the corpus callosum (Hudkins et al., 2012; Paul et al., 2008), and the right prefrontal lobe (Hudkins et al., 2012). On the other hand, some studies suggest that smoking decreases FA within the corpus callosum (Lin et al., 2013; Umene-Nakano et al., 2014) and left prefrontal cortex (Zhang et al., 2011). Several confounds may give rise to these inconsistent DTI findings including variable sample sizes, dissimilar inclusion criteria for smokers and matched controls, differing image acquisition and registration protocols, and varying statistical approaches.

Nonetheless, human imaging evidence does suggest the timing and volume of nicotine exposure exerts consistent effects on white matter characteristics. Over the long term, the total amount of nicotine consumed (or the severity of dependence) correlates negatively with FA in several brain regions (Hudkins et al., 2012; Liao et al., 2011; Lin et al., 2013; Paul et al., 2008; Umene-Nakano et al., 2014; Zhang et al., 2011). For example, Lin et al. (2013) found that the more years participants smoked, the lower the FA. Further, some studies have attempted to explain the variance in previous findings by a temporal model: nicotine exposure during adolescence increases FA values initially, but then chronic smoking throughout adulthood decreases FA (Hudkins et al., 2012; Paul et al., 2008). Over the short term, acute nicotine exposure via a

* Corresponding author. Tel.: +1 713 798 3502.
E-mail addresses: rsalas@bcm.edu, ramiritosalas@gmail.com (R. Salas).

http://dx.doi.org/10.1016/j.drugalcdep.2014.10.006
0376-8716/Published by Elsevier Ireland Ltd.

nicotine patch can increase FA within the corpus callosum, but only in participants with a low level of cotinine (Kochunov et al., 2013), a biomarker of nicotine exposure. These studies highlight that it is important to study a wide range of participants with varying smoking histories as well as controlling for acute nicotine exposures.

In the present study, we examined the effects of tobacco on white matter characteristics using four novel approaches. (1) To improve detection of white matter brain regions implicated, we acquired images with a greater number of diffusion gradient directions (71) than has been previously used in an attempt to more accurately fit the tensors in the DTI model. (2) We expanded whole-brain TBSS analyses to include not only FA measures as have been used previously (Lin et al., 2013; Umene-Nakano et al., 2014; Zhang et al., 2011) but also all standard tensor metrics as well as a crossing fiber model (Jbabdi et al., 2010) to better agnostically characterize the white matter alterations that arise from smoking. (3) We used probabilistic tractography to define subject specific tracts and compared DTI metrics within these tracts between smokers and healthy controls. (4) Finally, in a cohort of participants, we scanned smokers under two separate conditions: after smoking *as usual* and after abstinence (24 h). Although DTI metrics have been perceived to measure anatomically stable chronic characteristics, recent studies have shown acute changes after different manipulations (Hofstetter et al., 2013). DTI metrics have also been shown to change acutely as a result of nicotine administration via patch (Kochunov et al., 2013), but no DTI study to date has compared the same smokers while abstinent (asked to not smoke) and sated (allowed to smoke normally). Collectively, these approaches allowed us to further characterize the white matter changes in cigarette smokers.

2. Materials and methods

2.1. Participants

This study was approved by the Baylor College of Medicine institutional review board and participants were compensated for their time. 32 non-smokers and 30 cigarette smokers participated in the study. Participants were recruited from the greater Houston metropolitan area via advertisements. During phone screening callers who did not identify as treatment seeking, and smoked ≥10 cigarettes a day for at least one year were eligible for in-person screening. Non-smokers could not have smoked ≥5 cigarettes in their lifetime. Smokers were subject to an in-person screening interview and exclusion criteria for smokers included: other non-tobacco substance dependence, diagnosis of any AXIS I disorder according to the Mini-International Neuropsychiatric Interview, and a positive illicit drug urine toxicology at time of screening. Smokers were also required to give an exhaled breath carbon monoxide (CO) of ≥10 ppm on the day of smoking as usual, and ≤5 ppm on the day of abstinence. CO levels were measured using a CO meter (Micro + Smokerlyzer Monitor, Bedfont Scientific, Kent, England). Thirty cigarette smokers took part in the DTI scan when abstinent; of these, 15 participants returned to perform another identical DTI scan in which they smoked as usual prior to the scan.

To assess the level of nicotine dependence of smokers, we used the Fagerstrom Test for Nicotine Dependence (FTND), which consists of 6 questions with a mixture of multiple choice questions (scored 0–3) and yes/no questions (scored 0 or 1). The total score range is from 0 to 10, with 0 being lowest dependence and 10 being highest. The FTND was administered when smoking as usual.

2.2. Imaging acquisition details

All subjects were scanned on a Siemens 3T Trio Magnetom scanner at the Baylor College of Medicine's Center for Advanced Magnetic Resonance Imaging (CAMRI). Scanner acquisition parameters for the DTI sequence were as follows: voxel size: 2 mm × 2 mm × 2 mm, slices: 61 transversal slices (2 mm thick with no gap), phase encoding direction: A-P, FOV: 256 mm × 256 mm, TR: 9.4 s, TE: 91 ms, matrix size: 128 × 128, echo spacing: 73 ms, diffusion directions: 71 unique directions at $b_0 = 1000$ s/mm^2 with 8 repetitions at $b_0 = 0$ s/mm^2, duration: 12:32 m. Due to FOV and slice selection, the cerebellum and posterior occipital lobes were not fully captured for every subject.

2.3. Tract-based spatial statistics (TBSS)

To perform an unbiased, voxel-by-voxel analysis to identify WM regions with significantly different FA between non-smokers and smokers, we performed tract-based spatial statistics (TBSS) via FMRIB Software Library [FSL v5.0.4] (Jenkinson et al., 2012; Smith et al., 2006). The Neuroimaging in Python Interfaces and Pipelines (Nipype; Gorgolewski et al., 2011) was used to carry out the analyses and facilitate preprocessing. Raw diffusion weighted images (DWI) images were preprocessed first by correcting for motion artifacts by linearly registering each DWI volume to the first $b_0 = 0$ volume using FSL FLIRT (Jenkinson et al., 2002; Jenkinson and Smith, 2001) with 6 degrees of freedom (DOF) and appropriately rotating the *b*-vectors (Leemans and Jones, 2009). Second, the images were corrected for eddy current distortions using FSL's FMRIB's Diffusion Toolbox FDT (Behrens et al., 2003) *eddy_correct*. Next, the $8b_0 = 0$ volumes were averaged and then brain extracted (FSL *bet* (Smith, 2002)) to generate a brain mask. Diffusion tensors were fitted to the brain extracted DWI using FSL FDT (Behrens et al., 2003) *dtifit*. After preprocessing, all subjects' FA data were aligned into a common space using the nonlinear registration tool FNIRT (Andersson et al., 2007a,b), which uses a b-spline representation of the registration warp field (Rueckert et al., 1999). Next, the mean FA image was created and thinned to create a mean FA skeleton which represents the centers of all tracts common to the group. Each subject's aligned FA data was then projected onto this skeleton and the resulting data fed into voxel-wise cross-subject statistics. In addition to FA, TBSS was performed independently on axial diffusivity ($Da = \lambda_1$), radial diffusivity ($Dr = [\lambda_2 + \lambda_3]/2$), and mean diffusivity ($MD = [\lambda_1 + \lambda_2 + \lambda_3]/3$).

Between group comparisons were performed using permutations testing methods via FSL's *randomize* (Bullmore et al., 1999). All contrasts were run with 10,000 permutations and FSL's threshold-free cluster enhancement (TFCE) for clustering. Multiple-comparisons were corrected by controlling family-wise error (FWE), with significance thresholded at $p < 0.05$. Ethnicity, education, gender, and age were demeaned and entered as covariates in the GLM to isolate the effects of tobacco use. Furthermore, to explore how DTI measures correlated with these covariates directly, we also ran regressions with the individual covariates. Any regressions yielding significant voxels were then explored further to determine the effects of the covariates on their interaction with smoking status.

In addition to performing TBSS on traditional tensor measures (FA, Da, Dr, and MD), we also performed TBSS on crossing fiber measures. Tensor measures such as FA ignore information about fiber bundles and their orientations at each voxel. Recently, TBSS models have been extended to incorporate crossing fibers to measure relative structural integrity of multiple fibers along their principal direction at each voxel (Jbabdi et al., 2010). We used Bayesian sampling techniques (FSL *bedpostx*, default parameters) to build up the distribution of diffusion parameters on the basis of Markov Chain Monte Carlo (MCMC) sampling (Behrens et al., 2007). To compare fibers consistently across subjects, we used FSL *tbss_x* to align two fiber bundles at each voxel. We then proceeded to perform spatial statistics on each of the two fiber bundles, adjusting for covariates identical to the approach with tensor measures discussed above.

We also examined the impact of smoking dependence severity (as measured by FTND) on the TBSS. We used the FTND score as a regressor in the TBSS model described above for smokers to find voxels that correlate with FTND. All descriptive statistics were completed using MATLAB™. For all statistics with FTND and DTI, ethnicity, education, gender, and age were adjusted as regressors of no interest, as in all TBSS analyses.

2.4. Probabilistic tractography

While TBSS performs agnostic voxel-wise comparisons on major WM tracts common to all subjects, we also looked at particular tracts hypothesized to be implicated in nicotine dependent individuals. Specifically, we examined participant-specific tracts that connected to the frontal cortex from nucleus accumbens, habenula, and motor cortex.

We first used the Harvard-Oxford Cortical and Sub-cortical Structural probability atlases to generate seed masks for the nucleus accumbens (thresholded at >25%) and precentral gyrus (thresholded at >75%). These thresholds were selected to best isolate the two structures, as well as to use similar number of voxels in each seed (~1000 voxels). For the habenula, we isolated the center voxel in each subject's T1 anatomical image, drew a sphere with a radius of 3 mm around the voxel, and used boundary based linear registration (FSL *epi_reg*) to map the habenula ROIs into DWI space. For the target ROI, we generated a frontal cortex mask by including any coronal slices anterior to the temporal poles in MNI space. Each seed and target ROI was created for both hemispheres.

We then used probabilistic tractography (FSL *probtrackx2*) to find the WM tracts connecting each of the 6 seeds to the ipsilateral frontal cortex target ROI. We used default parameters for *probtrackx2* (5000 sample pathways, 0.2 curvature threshold, 2000 termination steps, 0.5 mm step length) and also incorporated 2 crossing fibers (*bedpostx*). Tractography was performed in subject's native diffusion space by back-projecting via inverting the non-linear transformations from diffusion to MNI space created by TBSS (FSL *tbss_deproject*). For each participant, each of the 6 generated tracts were first confined to white matter using the individual subject's white matter mask (generated by segmentation by FSL *fast*) and then thresholded to probabilities greater than 0.5% of the probabilistic index of connectivity (i.e., 0.005 × fdt_paths/waytotal). For each subject and tract, we then computed the spatially averaged FA within the thresholded tract and ran group statistics using a GLM model analogous to the model we used in TBSS. Thus, we could compare differences

Table 1
Demographic information and smoking severity measures.

	Controls Mean ± SD	Smokers Mean ± SD	
Education (years)	15.44 ± 2.6	13.47 ± 1.73***	
Gender	14 M; 18 F	17 M; 13 F	
Race	15 Caucasian 10 African American 1 Asian American 6 Hispanic	8 Caucasian 14 African American 0 Asian American 8 Hispanic	
Age (years)	35.97 ± 13.75	39.03 ± 9.90	
Years of smoking	N/A	21.15 ± 9.52 (obtained from 20 participants)	
FTND	N/A	5.37 ± 2.57	
Cigarettes/day	N/A	15.23 ± 7.68	
Exhaled CO (ppm)	N/A	15.17 ± 7.52 (smoking as usual)	3.21 ± 1.72 (abstinent 24 h)
Time since last cigarette (h)	N/A	2.33 ± 3.51 (smoking as usual)	26.92 ± 7.12 (abstinent 24 h)

*** $p < 0.001$ (two-sample, two-sided t-test).

in FA within our hypothesized tracts between controls, abstinent smokers, and sated smokers.

3. Results

3.1. Participants

Demographics for age, gender, race and smoking characteristics are shown in Table 1. Although we invited all 30 smokers to return for the second scan in which they smoked as usual prior to the scan, only 15 returned. Further, the FTND of the 15 participants who did return, had significantly greater FTND than the 15 participants who did not return (two-sample, two-way t-test: $p = 0.0020$, t-stat = 3.4099). The other smoking metrics (years of smoking, cigs/day, and exhaled CO) did not significantly differ between the two groups.

3.2. TBSS

3.2.1. Covariate interactions. Significant correlations were found between FA and two demographic covariates: gender and age. When gender was used as a covariate, females had several regions with significantly greater FA than males, and age negatively correlated with FA for several voxels throughout the brain ($p < 0.05$). Importantly, to test if gender and/or age had different impacts on smoking status, we regressed the age and gender covariates separately for smokers and non-smokers. No significant interactions were found between the two groups for either age or gender, indicating that the impact of gender and age are not significantly different for smokers and non-smokers.

3.2.2. FTND.. When FTND was regressed against FA in smokers, no voxels were found that had significant positive or negative correlation with FTND ($p > 0.25$, t-test, FWE corrected).

3.2.3. Controls vs. smokers (abstinent 24 h). Smokers (abstinent 24 h) had significantly decreased FA ($p < 0.05$, t-test, FWE corrected) compared to controls in several brain regions (Fig. 1). This reduction in FA in abstinent smokers was seen in the left and right splenium of the corpus callosum, with a larger region on the left side that extended more inferiorly. Reductions in FA were also found in smokers with bilateral anterior limb of the internal capsule. To better quantify the effect size of the reduction, we computed the mean of four DTI metrics (FA, MD, Dr, Da) within all significantly different voxels found by TBSS on FA (Fig. 2A). Within these regions, FA and Da decreased, while Dr and MD increased in smokers compared to controls. The mean FA within these regions in smokers correlated negatively with the number of years of regular smoking ($r^2 = 0.27$, $p < 0.05$). We also observed a positive trend in correlation of Dr and the number of years of regular smoking (Fig. 2B) that approached significance ($r^2 = 0.18$, $p = 0.054$). These correlations were run on data from 20 out of the 30 smokers from whom information on years of regular smoking was obtained. The correlations were weak, suggesting that many other factors may influence white matter disruptions; however, the correlation strengths and directions are consistent with previous findings (Lin et al., 2013).

3.2.4. Other DTI metrics: controls vs. smokers (abstinent 24 h). TBSS analysis also revealed changes in non-FA DTI metrics in abstinent smokers compared to controls. Smokers had higher Dr within the corpus callosum and internal capsule bilaterally (Fig. 3). Further, modeling the DTI data with 2 crossing fibers shows significant differences between smokers and controls in both fiber directions. Smokers showed decreases in anisotropy of the major fiber (F1) within notably large portions of the left corpus callosum (Fig. 4). Smokers also showed decreases in anisotropy of the second fiber (F2) within several anterior brain regions (Fig. 5). TBSS for Da and MD did not yield any significantly different voxels.

3.2.5. Sated vs. abstinent smokers. No differences in FA, MD, Dr, or Da were found via TBSS between smokers who smoked as usual (sated) and smokers who abstained for 24 h (abstinent).

3.3. Probabilistic tractography

3.3.1. Controls vs. smokers. Several differences between abstinent smokers (24 h) and controls were observed within the frontal-projecting white matter tracts (Fig. 6). When abstinent, smokers had lower FA in the right fronto-motor tract compared to controls ($p < 0.05$, GLM t-contrast control – smoker). When smoking as usual, smokers had lower FA compared to controls in left fronto-accumbal, right fronto-motor, and right fronto-habenula tracts ($p < 0.05$, GLM t-contrast control – smoker). When smoking as usual, smokers also had lower FA compared to abstinent smokers in right fronto-accumbal and right fronto-habenula tracts ($p < 0.05$, paired t-test).

3.3.2. Hemispheric asymmetry in smokers (abstinent 24 h). Previous studies (Lin et al., 2013) have shown asymmetrical disruptions in white matter as a result of smoking, with more disruptions in FA appearing on the left hemisphere. Our probabilistic tractography results also show that smokers (abstinent 24 h) have lower FA in the left fronto-habenula and left fronto-accumbal tracts compared to the right sided tracts ($p < 0.05$, paired t-test). However, control participants did not show any such asymmetry (Fig. 7).

4. Discussion

Our approaches yield three new pieces of evidence characterizing white matter disruptions from nicotine use: (1) Using TBSS, we found abstinent smokers compared to controls have decreased FA, increased radial diffusivity (Dr), and decreased anisotropy within aligned fiber bundles in several brain regions, including the corpus callosum and anterior internal capsule. (2) Structural connections were demonstrated between the frontal cortex and two reward-related brain areas (the nucleus accumbens (Balfour, 2002, 2004; Di Chiara et al., 2004) and the habenula (Salas et al., 2009; Velasquez

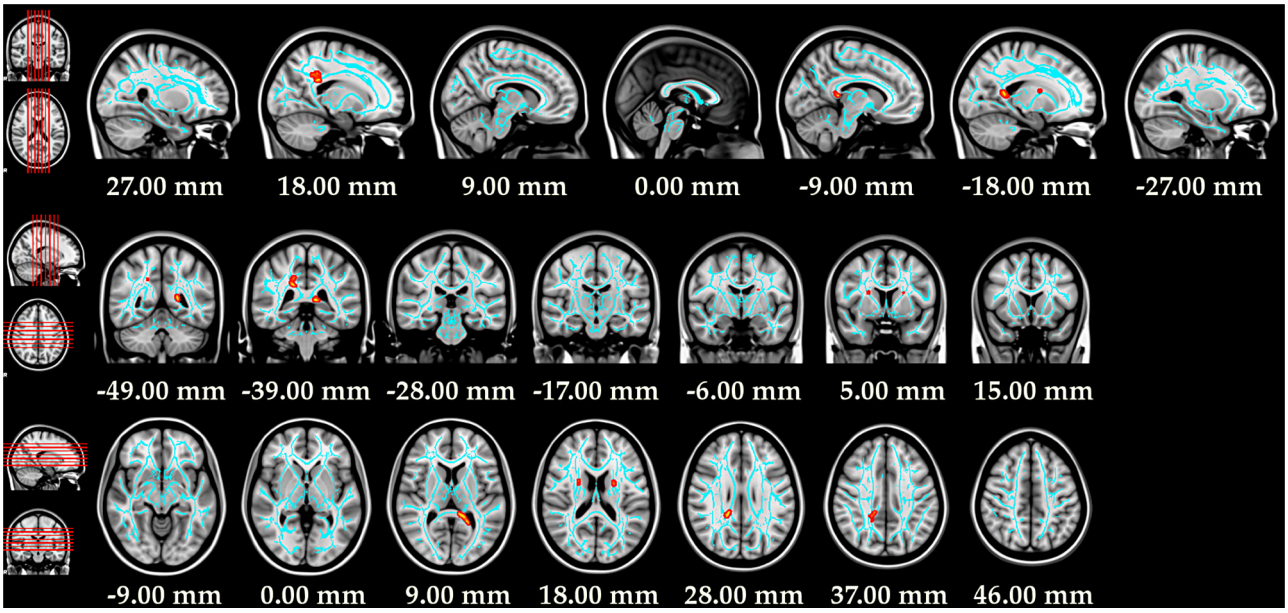

Fig. 1. TBSS results reveal that smokers have decreased FA in the L and R splenium of corpus callosum and the L and R anterior limb of internal capsule. Ethnicity, education, gender, and age were adjusted for as additional covariates in the GLM. Anatomical labels were derived from the JHU ICBM-DTI-81 White Matter Labels. The light blue indicates the skeletonized WM in which the voxel-wise TBSS was performed. The red-yellow shows significant voxels ($p < 0.05$, FWE controlled) with the voxels filled along the WM tracts for easier visibility. Brain images are in radiologic convention (right hemisphere appears on left).

et al., 2014)) to be implicated in chronic nicotine smoking, and these disruptions were further exaggerated by acute smoking. (3) We found specific hemispheric asymmetries within frontal projecting tracts observed in chronic smokers but not in healthy controls, suggesting the white matter disruptions in the left hemisphere to be more susceptible to the effects of nicotine than the right hemisphere. Collectively, our study uses recent DTI approaches to better characterize the adverse effects of nicotine on white matter characteristics in the brain.

First, using TBSS the current results show decreased FA within regions of the corpus callosum, in line with more recent studies (Lin et al., 2013; Umene-Nakano et al., 2014) and refuting older ones (Hudkins et al., 2012; Paul et al., 2008). Also using TBSS, we found Dr was increased in the corpus callosum in smokers (abstinent 24 h) compared to controls, a result that was previously not found (Umene-Nakano et al., 2014) or not explicitly searched for using TBSS (Lin et al., 2013). We also built a model that incorporated crossing fibers (Jbabdi et al., 2010) and found large decreases in anisotropy along the first fiber direction in the entirety of the left corpus callosum and decreased anisotropy in several frontal WM regions in bilateral frontal regions. Such a model had not been tested for nicotine dependence, and our analysis with this model supports previous studies reporting left sided corpus callosum disruptions in smokers (Lin et al., 2013). Further, by aligning fiber orientations and running TBSS on each fiber bundle individually, we were also able to elucidate decreases in anisotropy in anterior internal capsule and frontal regions, a result not previously reported in TBSS analyses on FA only. Our data also recapitulated correlations of FA and years of nicotine use previously seen across several studies (Hudkins et al., 2012; Liao et al., 2011; Lin et al., 2013; Paul et al., 2008; Umene-Nakano et al., 2014; Zhang et al., 2011). Although the directionality of the correlations are consistent with the literature, all studies including our own have used relatively small sample sizes. The strength of these mild correlations might be increased by: (1) using an order of magnitude greater number of smokers, (2) adjusting for further demographic and biological data (e.g. socioeconomic conditions, genetic predispositions), and (3) acquiring better estimates of total lifetime volume of nicotine exposure. In sum, our TBSS data further elucidate the changes seen within the corpus callosum and the anterior limb of the internal capsule seen in cigarette smokers but not in controls.

Second, the probabilistic tractography within our 3 hypothesized tracts (fronto-accumbal, fronto-habenular, and fronto-motor) revealed a general trend of decreasing FA in smokers who abstained from smoking for 24 h, compared to controls. These changes were further exacerbated when smokers smoked as usual (sated). Even though our TBSS analysis did not reveal any differences between smoking as usual and abstinent smokers, we found the right fronto-habenula and fronto-accumbal tracts to be decreased further when smokers recently smoked. We also found 3 of the 6 tracts to show significantly lower FA in sated smokers compared to controls. Using subject-specific tracts to perform statistics rather than common group approaches like TBSS can reveal more subtle differences that can wash away in spatial normalization. Further, we also found evidence for hemispheric asymmetry in which the left hemisphere contained more disruptions in smokers but not controls, a result supporting previously observed findings (Lin et al., 2013). Although previous studies found significant correlations between FTND and DTI metrics (Hudkins et al., 2012; Paul et al., 2008; Zhang et al., 2011), our data did not show such correlations using two different approaches.

Third, the probabilistic tractography results in this paper support the hypothesis that acute effects of nicotine enhance the observable chronic disruptions in DTI in smokers in some regions. The opposite hypothesis, for smokers to show increases in FA after recent use, is also plausible and has been previously observed in the genu of the corpus callosum after recent nicotine administration (Kochunov et al., 2013) and in smokers who recently began smoking (Hudkins et al., 2012; Liao et al., 2011; Lin et al., 2013). Support for this hypothesis stems from the presence of functional nicotinic acetylcholine receptors (nAChRs) within the white matter of the brain (Ding et al., 2004; Kochunov et al., 2013; Pimlott et al., 2004; Vizi and Lendvai, 1999) and/or glial swelling (Hudkins et al., 2012; Opanashuk et al., 2001), which could account for acute exposure to nicotine increasing FA values. Our results show that smokers who

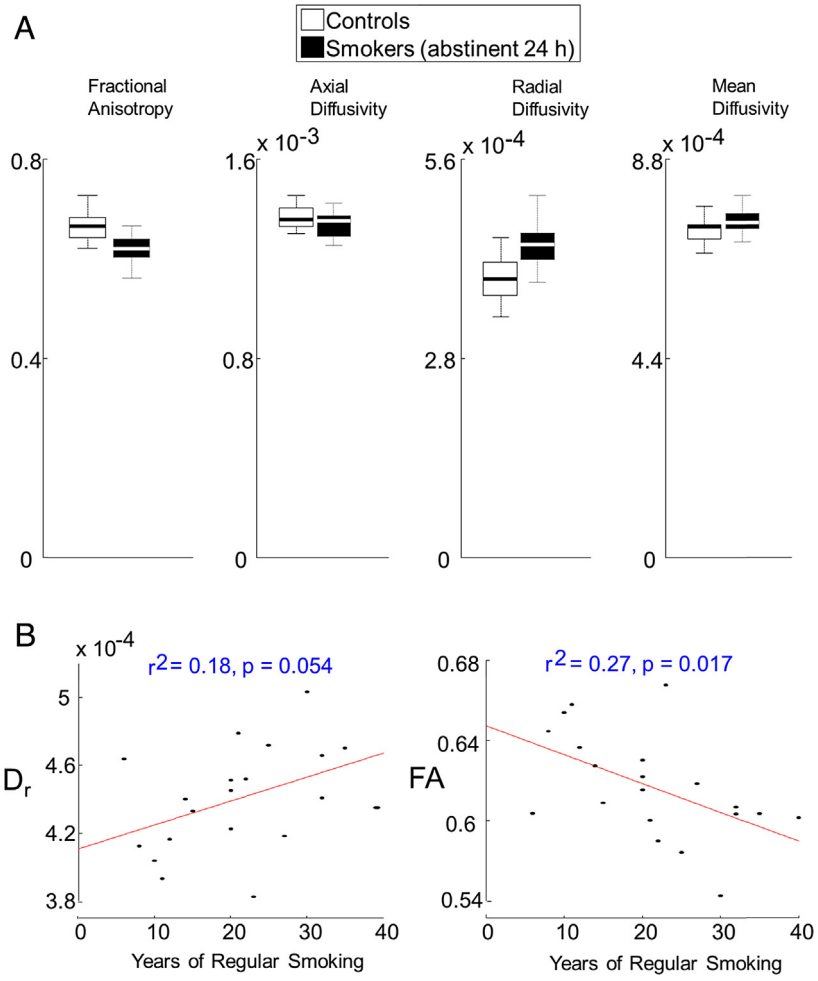

Fig. 2. WM regions with significantly lower FA in smokers also show changes in other DTI measures. (A) FA was decreased, Da was decreased, Dr was increased, and MD was increased in smokers compared to non-smokers. Significance testing was not computed here to avoid circularity. The box and whisker plots show group statistics of the averaged DTI metrics from each tract: median within the box, the 25th and 75th percentiles at the bounds of the box, the extremes of the data not outliers as whiskers, and the outliers in red crosses. (B) Correlations of DTI metrics with severity of smoking revealed a negative correlation of FA and duration of smoking and a positive correlation with Dr and duration of smoking. Data is from 20 of the 30 smokers from which years of regular smoking was obtained. These characteristic correlations are highly consistent with Lin et al. (2013), even though our brain regions differ.

were sated had decreases in FA compared to the same smokers when they abstained for 24 h within particular frontal projecting tracts. Since our TBSS results showed no difference between sated and abstinent smokers, it is possible that acute nicotine exposure affects only specific WM tracts. Further, smokers exhibited greater disruptions in the left compared to right tracts. Although we did not hypothesize such a laterality difference selectively in smokers, the greater DTI changes in the left hemisphere may parallel lateralization of dopaminergic systems. Dopaminergic dysfunction is characteristic in Parkinson's disease, in which greater nigrostriatal damage is seen on the left hemisphere (Scherfler et al., 2012) and in which stronger left lateralized functional connectivity is

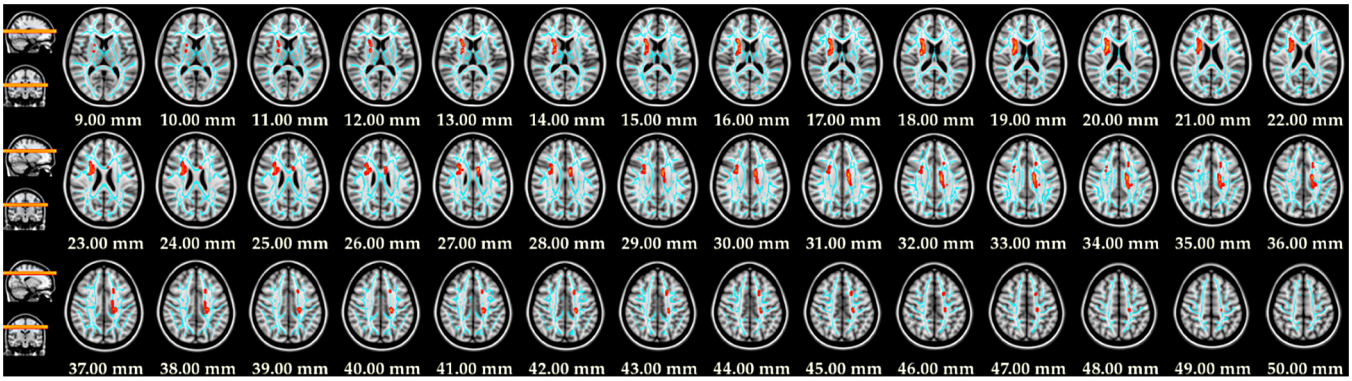

Fig. 3. TBSS results reveal smokers have increased Dr diffusely in corpus callosum and bilateral internal capsule. Ethnicity, education, gender, and age were adjusted for as additional covariates in the GLM. Anatomical labels were derived from the JHU ICBM-DTI-81 White Matter Labels.

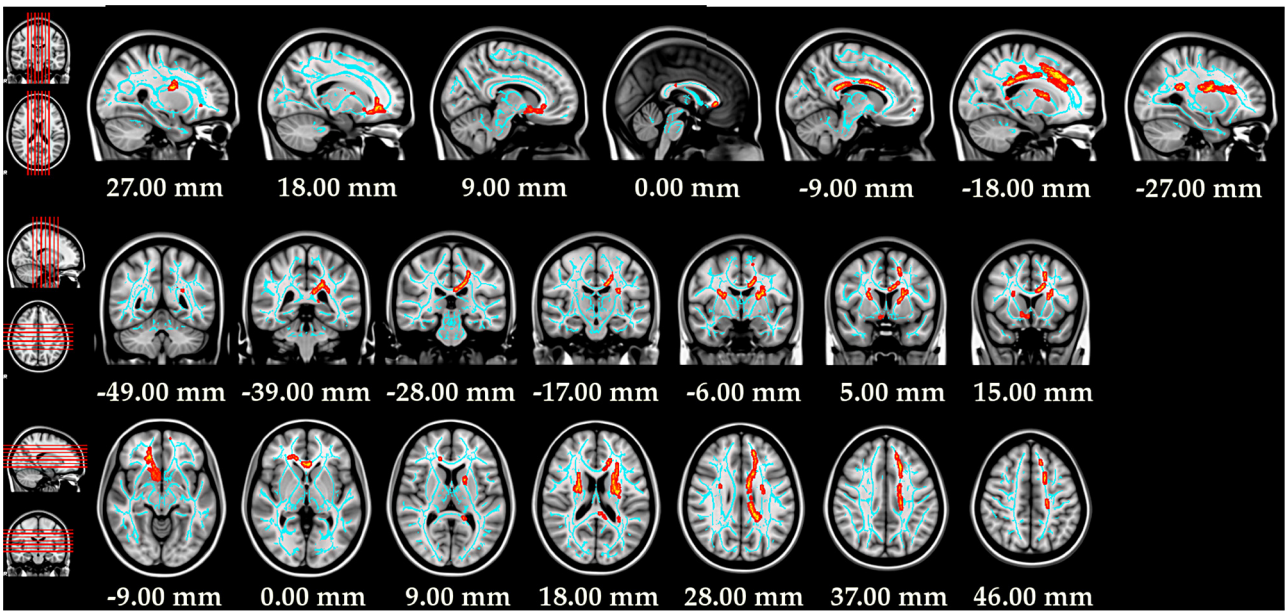

Fig. 4. TBSS results reveal smokers have significantly decreased anisotropy along the major fiber (F1) in the L body of the corpus callosum (top row), the bilateral anterior limb of the internal capsule (middle row), and the L forceps minor (bottom row). Ethnicity, education, gender, and age were adjusted for as additional covariates in the GLM. Anatomical labels were derived from the JHU ICBM-DTI-81 White Matter Labels or the JHU White-Matter Tractography atlas.

associated with a decreased risk for Parkinson's disease (Ellmore et al., 2013). This is further supported by the fact that smoking propensity can be altered in humans via dopaminergic agonists and inverse agonists (Caskey et al., 2002). Interestingly, we also did not hypothesize the fronto-motor tracts to differ significantly from controls or between abstinent and sated smokers. However, disruptions in motor coordination have been observed in rats with prenatal exposure to tobacco extracts (Khalki et al., 2012), suggesting the motor circuit may also be implicated in nicotine use. Further, nicotine exposure may induce changes to networks throughout the frontal cortex, giving rise to our observed changes in all three frontal projecting tracts.

An alternative interpretation of the data is that the white matter changes in the abstinent smokers are related to acute withdrawal of nicotine rather than chronic nicotine exposure. This seems plausible, as 24 h without a cigarette certainly induces withdrawal symptoms (Thompson-Lake et al., 2014). However, we did not find significant differences in the paired TBSS analysis of smokers in sated vs. abstinent conditions. Further, our probabilistic tractography data show that when sated, the FA measures decline further rather than reversing, as would be expected if the effect was due to withdrawal. That is, we did not observe FA measures to restore towards the level of controls when smokers recently smoked. Nonetheless, a further investigation parametrically modulating

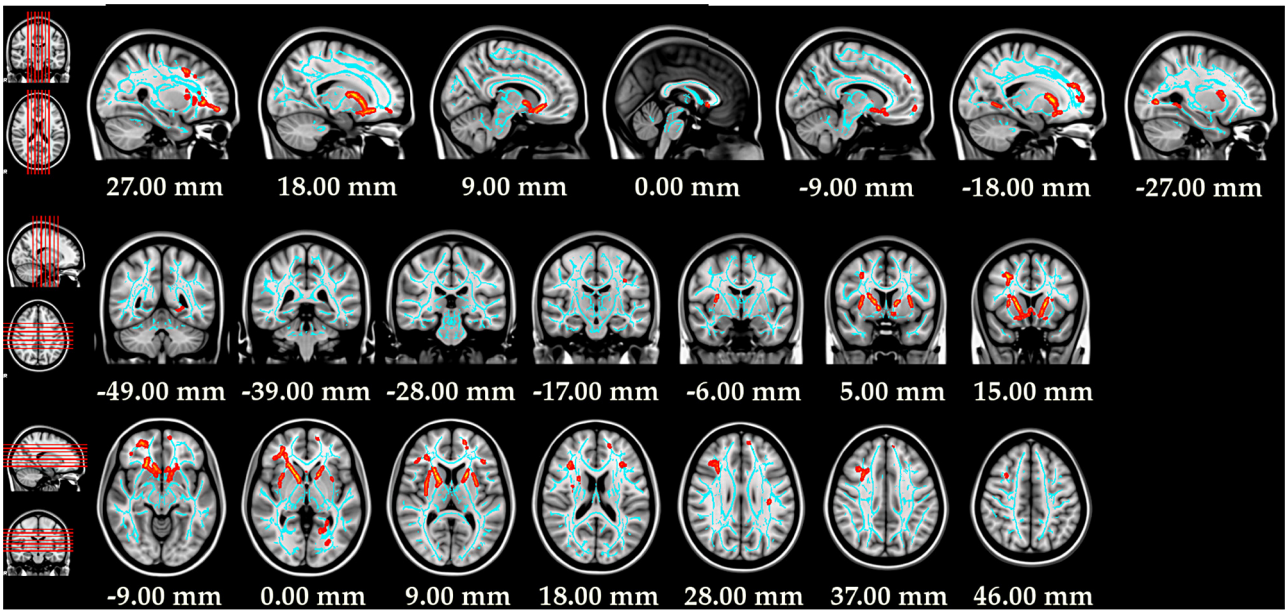

Fig. 5. TBSS results reveal smokers have significantly decreased diffusivity along the second anistropy (F2) in bilateral anterior internal capsule (top row), the L inferior fronto-occipital fasciculus (middle row), and the R genu of the corpus callosum (bottom row). Ethnicity, education, gender, and age were adjusted for as additional covariates in the GLM. Anatomical labels were derived from the JHU ICBM-DTI-81 White Matter Labels or the JHU White-Matter Tractography atlas.

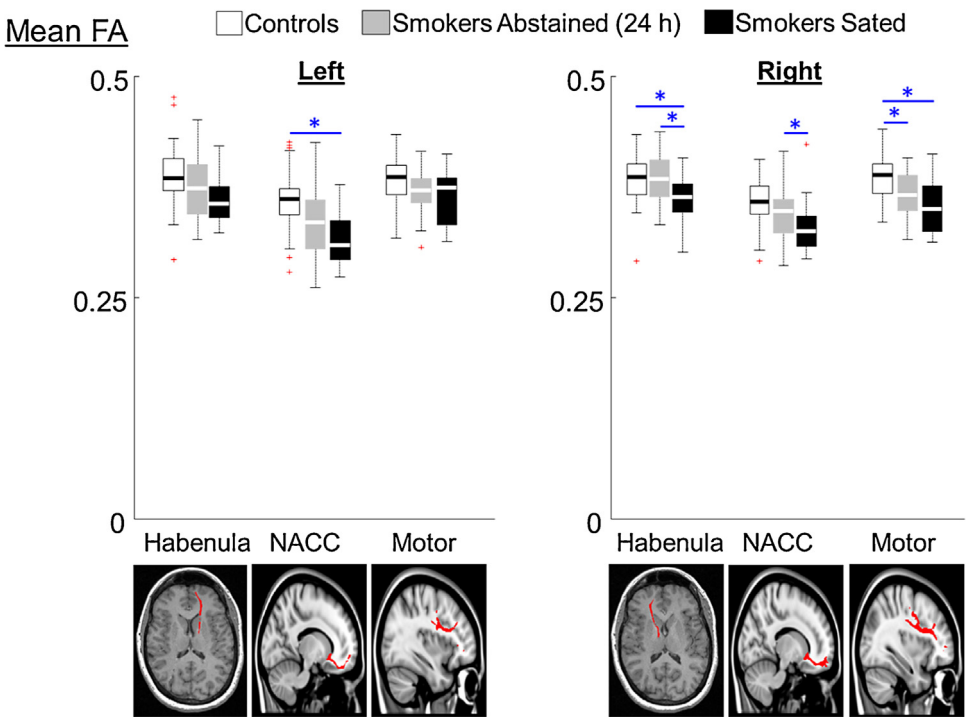

Fig. 6. Chronic tobacco use causes decreases in FA within frontal projecting tracts, which show further decreases in FA when smokers have recently smoked. Probabilistic tractography was used to find specific tracts projecting to the frontal cortex originating from 3 ROIs: habenula, nucleus accumbens (NACC), and pre-central gyrus (motor). Tracts from a representative participant are shown on the bottom row of images corresponding to the ROI seeds. Above each image is the distribution of FA across subjects within that tract. The box and whisker plots show group statistics of the averaged FA from each tract: median within the box, the 25th and 75th percentiles at the bounds of the box, the extremes of the data not outliers as whiskers, and the outliers in red crosses.

the duration of abstinence and observing the effects on DTI metrics might further substantiate our findings.

The characteristics of the altered DTI metrics in smokers may elucidate the biological underpinnings of the impact of nicotine on white matter. Smokers were found to have an increase in radial diffusivity compared to controls without significant decreases in axial diffusivity, suggesting the disruptions observed in smokers are more likely related to dysmyelinated axons rather than axonal injury (Song et al., 2003, 2002, 2005). This finding is consistent with rodent studies that revealed gestational nicotine exposure decreased myelin gene expression in both adolescent and adult rats in regions including the prefrontal cortex, basal ganglia, and the nucleus accumbens (Cao et al., 2013a,b).

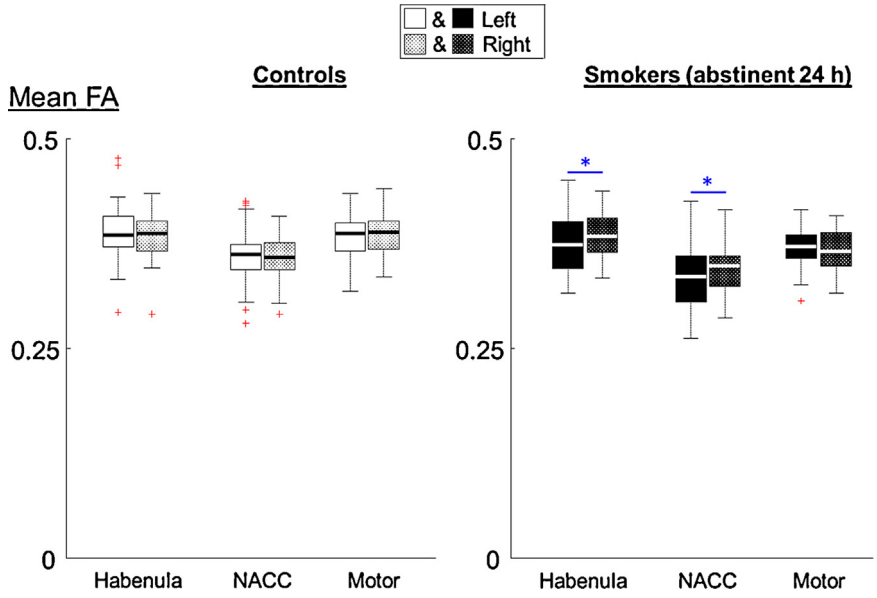

Fig. 7. Nicotine users show asymmetrical hemispheric differences in FA along fronto-habenula and fronto-accumbal tracts. Nicotine users showed significantly lower FA (*$p < 0.05$, paired t-test) along the L habenulo-frontal and accumbo-frontal tracts compared to the corresponding right hemispheric tract. Controls showed no hemispheric asymmetries along any of our measured tracts. The box and whisker plots show the group statistics of the averaged FA from each tract: median within the box, the 25th and 75th percentiles at the bounds of the box, the extremes of the data not outliers as whiskers, and the outliers in red crosses.

Our study has four important limitations. First, our DTI sequence prevented imaging of the cerebellum and the posterior occipital lobe, limiting inferences from these regions. Further, incomplete imaging of the cerebellum could prevent optimal image registration. Second, we did not scan control subjects twice to measure the test–retest reliability of the imaging as well as the analysis approaches. This is a growing concern in DTI imaging, and TBSS approaches are subject to imperfect test–retest reliability (Madhyastha et al., 2014). Third, we did not randomize the days that smokers were abstinent. Due to participation in a separate study (a virtual reality session prior to scanning), all subjects had been abstinent for over 24 h on the first day they were scanned. Further, the 15 participants who did return for the second scan while smoking as usual had significantly greater FTND. This may limit the implications of the effects of acute nicotine exposure on DTI metrics to smokers who have a greater dependence on nicotine. Fourth, there are a multitude of factors that could additionally or partially explain differences in DTI metrics between controls and smokers. Our covariates accounted for linear trends in the data; however, non-linear effects of age and education in particular were not removed. Further, we did not assess other indices of health including but not limited to: diabetes, blood pressure, hypertension, and cardiac disorders. Thus, our study cannot state that tobacco plays any causal role on these observed changes, only that a correlation was observed.

Our study investigated the effects of nicotine use on white matter characteristics using a variety of approaches. By using multiple directions in our DTI image acquisition and incorporating crossing fibers into our TBSS analysis, we provide a more complete picture of white matter disruptions in chronic smokers, including regions of decreased FA in the corpus callosum. Further, our probabilistic tractography data reveals decreases in FA in smokers in white matter tracts projecting to the frontal cortex from the nucleus accumbens, habenula, and the motor cortex. Disruptions were greater on the left side in smokers vs. non-smokers, and decreases were generally exaggerated by acute exposure to cigarette smoking. DTI may help elucidate the addictive potential of nicotine and how it interacts with cortical and subcortical white matter. Fortunately, there is some evidence that quitting smoking for >20 years restores disruptions in white matter characteristics (Gons et al., 2011), suggesting these disruptions may not be permanent. Mapping what the disruptions are and how they can recover could be instrumental in therapeutic development.

Role of funding source

This work was supported by NIH grants DA026539 and DA09167 to RS. Additional funding and support was provided by the McNair Medical Institute, the Brain and Behavior Research Foundation (NARSAD), and the Diana Helis Henry Medical Research Foundation through its direct engagement in the continuous active conduct of medical research in conjunction with the Baylor College of Medicine Menninger Clinic, the Department of Psychiatry, and the Duncan Cancer Center. The funding sources had no role on the design, implementation, or analysis of these experiments.

Contributors

Study concept and design: Dr. De La Garza, Dr. Eagleman, Dr. Philip Baldwin and Dr. Salas. Participant recruitment: Daisy Thompson-Lake and Kenia Velazquez. Image Acquisition: Kenia Velazquez. Data Analysis: Ricky Savjani and Dr. Salas. Writing manuscript: Ricky Savjani and Dr. Salas. All authors have read, edited, and approved the submitted and revised versions of this manuscript.

Conflict of interest

No conflict declared.

Acknowledgements

We thank Eduardo Aramayo for technical assistance and Pablo Ormachea for assisting in the writing of this manuscript. We thank the Baylor College of Medicine Computational and Integrative Biomedical Research (CIBR) center for providing software licenses and access to cluster computing resources and the McNair Initiative for Neuroscience Discovery – Menninger/Baylor (MIND-MB) project.

References

Andersson, J.L.R., Jenkins, M., Smith, S., 2007a. Non-linear Optimisation. In: FMRIB Analysis Group Technical Rreport TR07JA1.
Andersson, J.L.R., Jenkins, M., Smith, S., 2007b. Non-linear Registration, aka Spatial Normalisation FMRIB Analysis Group Technical Report TR07JA2.
Balfour, D.J., 2002. Neuroplasticity within the mesoaccumbens dopamine system and its role in tobacco dependence. Curr. Drug Targets CNS Neurol. Disord. 1, 413–421.
Balfour, D.J., 2004. The neurobiology of tobacco dependence: a preclinical perspective on the role of the dopamine projections to the nucleus accumbens [corrected]. Nicotine Tob. Res. 6, 899–912.
Behrens, T.E., Berg, H.J., Jbabdi, S., Rushworth, M.F., Woolrich, M.W., 2007. Probabilistic diffusion tractography with multiple fibre orientations: what can we gain? Neuroimage 34, 144–155.
Behrens, T.E., Woolrich, M.W., Jenkinson, M., Johansen-Berg, H., Nunes, R.G., Clare, S., Matthews, P.M., Brady, J.M., Smith, S.M., 2003. Characterization and propagation of uncertainty in diffusion-weighted MR imaging. Magn. Reson. Med. 50, 1077–1088.
Bullmore, E.T., Suckling, J., Overmeyer, S., Rabe-Hesketh, S., Taylor, E., Brammer, M.J., 1999. Global, voxel, and cluster tests, by theory and permutation, for a difference between two groups of structural MR images of the brain. IEEE Trans Med. Imaging 18, 32–42.
Cao, J., Dwyer, J.B., Gautier, N.M., Leslie, F.M., Li, M.D., 2013a. Central myelin gene expression during postnatal development in rats exposed to nicotine gestationally. Neurosci. Lett. 553, 115–120.
Cao, J., Wang, J., Dwyer, J.B., Gautier, N.M., Wang, S., Leslie, F.M., Li, M.D., 2013b. Gestational nicotine exposure modifies myelin gene expression in the brains of adolescent rats with sex differences. Transl. Psychiatry 3, e247.
Caskey, N.H., Jarvik, M.E., Wirshing, W.C., Madsen, D.C., Iwamoto-Schaap, P.N., Eisenberger, N.I., Huerta, L., Terrace, S.M., Olmstead, R.E., 2002. Modulating tobacco smoking rates by dopaminergic stimulation and blockade. Nicotine Tobacco Res. 4, 259–266.
Di Chiara, G., Bassareo, V., Fenu, S., De Luca, M.A., Spina, L., Cadoni, C., Acquas, E., Carboni, E., Valentini, V., Lecca, D., 2004. Dopamine and drug addiction: the nucleus accumbens shell connection. Neuropharmacology 47 (Suppl. 1), 227–241.
Ding, Y.S., Fowler, J.S., Logan, J., Wang, G.J., Telang, F., Garza, V., Biegon, A., Pareto, D., Rooney, W., Shea, C., Alexoff, D., Volkow, N.D., Vocci, F., 2004. 6-[^{18}F]Fluoro-A-85380, a new PET tracer for the nicotinic acetylcholine receptor: studies in the human brain and in vivo demonstration of specific binding in white matter. Synapse 53, 184–189.
Ellmore, T.M., Castriotta, R.J., Hendley, K.L., Aalbers, B.M., Furr-Stimming, E., Hood, A.J., Suescun, J., Beurlot, M.R., Hendley, R.T., Schiess, M.C., 2013. Altered nigrostriatal and nigrocortical functional connectivity in rapid eye movement sleep behavior disorder. Sleep 36, 1885–1892.
Gons, R.A., van Norden, A.G., de Laat, K.F., van Oudheusden, L.J., van Uden, I.W., Zwiers, M.P., Norris, D.G., de Leeuw, F.E., 2011. Cigarette smoking is associated with reduced microstructural integrity of cerebral white matter. Brain 134, 2116–2124.
Gorgolewski, K., Burns, C.D., Madison, C., Clark, D., Halchenko, Y.O., Waskom, M.L., Ghosh, S.S., 2011. Nipype: a flexible, lightweight and extensible neuroimaging data processing framework in python. Front. Neuroinform. 5, 13.
Hofstetter, S., Tavor, I., Tzur Moryosef, S., Assaf, Y., 2013. Short-term learning induces white matter plasticity in the fornix. Neuroscience 33, 12844–12850.
Hudkins, M., O'Neill, J., Tobias, M.C., Bartzokis, G., London, E.D., 2012. Cigarette smoking and white matter microstructure. Psychopharmacology 221, 285–295.
Jbabdi, S., Behrens, T.E., Smith, S.M., 2010. Crossing fibres in tract-based spatial statistics. Neuroimage 49, 249–256.
Jenkinson, M., Bannister, P., Brady, M., Smith, S., 2002. Improved optimization for the robust and accurate linear registration and motion correction of brain images. Neuroimage 17, 825–841.
Jenkinson, M., Beckmann, C.F., Behrens, T.E., Woolrich, M.W., Smith, S.M., 2012. FSL. Neuroimage 62, 782–790.
Jenkinson, M., Smith, S., 2001. A global optimisation method for robust affine registration of brain images. Med. Image Anal. 5, 143–156.

Khalki, H., Khalki, L., Aboufatima, R., Ouachrif, A., Mountassir, M., Benharref, A., Chait, A., 2012. Prenatal exposure to tobacco extract containing nicotinic alkaloids produces morphological and behavioral changes in newborn rats. Pharmacol. Biochem. Behav. 101, 342–347.

Kochunov, P., Du, X., Moran, L.V., Sampath, H., Wijtenburg, S.A., Yang, Y., Rowland, L.M., Stein, E.A., Hong, L.E., 2013. Acute nicotine administration effects on fractional anisotropy of cerebral white matter and associated attention performance. Front. Pharmacol. 4, 117.

Leemans, A., Jones, D.K., 2009. The B-matrix must be rotated when correcting for subject motion in DTI data. Magn. Reson. Med. 61, 1336–1349.

Liao, Y., Tang, J., Deng, Q., Deng, Y., Luo, T., Wang, X., Chen, H., Liu, T., Chen, X., Brody, A.L., Hao, W., 2011. Bilateral fronto-parietal integrity in young chronic cigarette smokers: a diffusion tensor imaging study. PLoS ONE 6, e26460.

Lin, F., Wu, G., Zhu, L., Lei, H., 2013. Heavy smokers show abnormal microstructural integrity in the anterior corpus callosum: a diffusion tensor imaging study with tract-based spatial statistics. Drug Alcohol Depend. 129, 82–87.

Madhyastha, T., Merillat, S., Hirsiger, S., Bezzola, L., Liem, F., Grabowski, T., Jancke, L., 2014. Longitudinal reliability of tract-based spatial statistics in diffusion tensor imaging. Hum. Brain Mapp. 35, 4544–4555.

Opanashuk, L.A., Pauly, J.R., Hauser, K.F., 2001. Effect of nicotine on cerebellar granule neuron development. Eur. J. Neurosci. 13, 48–56.

Paul, R.H., Grieve, S.M., Niaura, R., David, S.P., Laidlaw, D.H., Cohen, R., Sweet, L., Taylor, G., Clark, R.C., Pogun, S., Gordon, E., 2008. Chronic cigarette smoking and the microstructural integrity of white matter in healthy adults: a diffusion tensor imaging study. Nicotine Tob. Res. 10, 137–147.

Pimlott, S.L., Piggott, M., Owens, J., Greally, E., Court, J.A., Jaros, E., Perry, R.H., Perry, E.K., Wyper, D., 2004. Nicotinic acetylcholine receptor distribution in Alzheimer's disease, dementia with Lewy bodies, Parkinson's disease, and vascular dementia: in vitro binding study using 5-[(125)i]-a-85380. Neuropsychopharmacology 29, 108–116.

Rueckert, D., Sonoda, L.I., Hayes, C., Hill, D.L., Leach, M.O., Hawkes, D.J., 1999. Nonrigid registration using free-form deformations: application to breast MR images. IEEE Trans. Med. Imaging 18, 712–721.

Salas, R., Sturm, R., Boulter, J., De Biasi, M., 2009. Nicotinic receptors in the habenulo-interpeduncular system are necessary for nicotine withdrawal in mice. J. Neurosci. 29, 3014–3018.

Scherfler, C., Seppi, K., Mair, K.J., Donnemiller, E., Virgolini, I., Wenning, G.K., Poewe, W., 2012. Left hemispheric predominance of nigrostriatal dysfunction in Parkinson's disease. Brain 135, 3348–3354.

Smith, S.M., 2002. Fast robust automated brain extraction. Hum. Brain Mapp. 17, 143–155.

Smith, S.M., Jenkinson, M., Johansen-Berg, H., Rueckert, D., Nichols, T.E., Mackay, C.E., Watkins, K.E., Ciccarelli, O., Cader, M.Z., Matthews, P.M., Behrens, T.E., 2006. Tract-based spatial statistics: voxelwise analysis of multi-subject diffusion data. Neuroimage 31, 1487–1505.

Song, S.K., Sun, S.W., Ju, W.K., Lin, S.J., Cross, A.H., Neufeld, A.H., 2003. Diffusion tensor imaging detects and differentiates axon and myelin degeneration in mouse optic nerve after retinal ischemia. Neuroimage 20, 1714–1722.

Song, S.K., Sun, S.W., Ramsbottom, M.J., Chang, C., Russell, J., Cross, A.H., 2002. Dysmyelination revealed through MRI as increased radial (but unchanged axial) diffusion of water. Neuroimage 17, 1429–1436.

Song, S.K., Yoshino, J., Le, T.Q., Lin, S.J., Sun, S.W., Cross, A.H., Armstrong, R.C., 2005. Demyelination increases radial diffusivity in corpus callosum of mouse brain. Neuroimage 26, 132–140.

Thompson-Lake, D.G.Y., Cooper, K.N., Mahoney III, J.J., Bordnick, P.S., Salas, R., Kosten, T.R., Dani, J.A., De La Garza II, R., 2014. Withdrawal symptoms and nicotine dependence severity predict virtual reality craving in cigarette deprived smokers. Nicotine and Tobacco Research (in press).

Umene-Nakano, W., Yoshimura, R., Kakeda, S., Watanabe, K., Hayashi, K., Nishimura, J., Takahashi, H., Moriya, J., Ide, S., Ueda, I., Hori, H., Ikenouchi-Sugita, A., Katsuki, A., Atake, K., Abe, O., Korogi, Y., Nakamura, J., 2014. Abnormal white matter integrity in the corpus callosum among smokers: tract-based spatial statistics. PLoS ONE 9, e87890.

Velasquez, K.M., Molfese, D.L., Salas, R., 2014. The role of the habenula in drug addiction. Front. Hum. Neurosci. 8, 174.

Vizi, E.S., Lendvai, B., 1999. Modulatory role of presynaptic nicotinic receptors in synaptic and non-synaptic chemical communication in the central nervous system. Brain Res. Brain Res. Rev. 30, 219–235.

Zhang, X., Salmeron, B.J., Ross, T.J., Geng, X., Yang, Y., Stein, E.A., 2011. Factors underlying prefrontal and insula structural alterations in smokers. Neuroimage 54, 42–48.